# NORTHWESTERN UNIVERSITY

## McCORMICK SCHOOL OF ENGINEERING AND APPLIED SCIENCE

## DEPARTMENT OF MATERIALS SCIENCE AND ENGINEERING

TECHNICAL REPORT #33

OCTOBER 1992

OFFICE OF NAVAL RESEARCH

CONTRACT NO. N00014-80-C-116

# SOME RECENT RESULTS ON STRESSES IN THIN FILMS AND PRECIPITATES



BY

J. B. COHEN



EVANSTON, ILLINOIS

# SOME RECENT RESULTS ON STRESSES IN THIN FILMS AND PRECIPITATES

J. B. Cohen
Department of Materials Science and Engineering
McCormick School of Engineering
Northwestern University
Evanston, IL 60202

## Abstract

Diffraction remains the premier tool for sampling the residual stresses in materials non destructively, the only one capable of determining the entire stress tensor, and with few assumptions. The technique has kept pace with the needs of researchers in the area of multiphase materials; now, the stresses can be separated into macro and micro components. The deviatoric macro and micro stress components and hydrostatic macrostress can be measured without knowledge of the unstressed lattice parameter. Bond strength of film and fiber and the yield stress can be examined by cooling samples, and there are new developments that enable gradients to be determined.

## Introduction

Residual stresses can play an important role in a material's properties and performance -- from miniature solid state devices to railroad ties, pipelines and even in large telescope mirrors (1,2,3). While there are a host of techniques for measuring stress, destructively or non destructively, none approach the detail and versatility possible with diffraction of x-rays or neutrons, and to illustrate the techniques and this versatility is the purpose of this paper.

Generally, we can speak of the ability to measure of two kinds of stresses in materials -- macro and microstresses. Macrostresses are the stresses traditionally measured by dissection -- the kind that would develop in a truly homogeneous material, of which there are few, if any. It is often said that these are the only stresses about which an engineer is really interested, but we shall see that this is not the case at all.

Macrostresses typically arise in a material from different amounts of plastic flow in different regions of a material. For example, in bending, the outer layers may deform plastically, while the region near the central axis is deforming elastically. When released there is a gradient in stress throughout the beam, but the stress sums to zero across a sectional area,

$$\int_V \sigma_{ij}\, dA = 0 \qquad (1)$$

Furthermore,

$$\sigma_{1j,j} = 0 \qquad (2a)$$

or:

$$\frac{\partial \sigma_{13}}{\partial x_1} + \frac{\partial \sigma_{23}}{\partial x_2} + \frac{\partial \sigma_{33}}{\partial x_3} = 0 \qquad (2b)$$

Here $x_1$ and $x_2$ are orthogonal axes on the surface and $x_3$ is normal to it. As the macro stresses are assumed to be uniform in a surface, the first two terms are zero and therefore the last term is zero. There is no gradient and $\sigma_{33}$ must have the same value in the bulk as in the surface. Another condition is that in the absence of applied loads at any point:

$$\sigma_{ij} \bullet n_j = 0 \qquad (3)$$

where $n_i$ is normal to the surface. Now , this means that $\sigma_{33} \bullet n_3 = 0$, or $\sigma_{33} = 0$ at the surface and hence internally as well. Similarly it can be shown that for macrostresses, $\sigma_{23} = \sigma_{13} = 0$ as well.

The microstresses arise from microscopic inhomogeneity from the elastic anisotropy of a grain in a polycrystalline array, from the differences in yield of one grain with respect to its neighbors, etc. Such phenomena can occur in a single phase material, and in a multiphase material they can arise from the difference in elastic or plastic properties of the different phases. These stresses must average to zero over the entire volume.

$$\int \sigma_{ij} dV = 0 \qquad (4)$$

From this equation, for a two phase material, the <u>microstresses</u> in both phases balance (2):

$$(1-f) < {}^{\mu}\sigma_{ij} >_{matrix} + < {}^{\mu}\sigma_{ij} >_{ppt} = 0 \qquad (5)$$

The carats imply averaging over the measuring volume and f is the volume fraction. This equation can be extended to any number of phases. Furthermore, $\sigma_{i3}$ terms can exist in this case, since these microstresses do vary from point to point. They can be detected since diffraction samples not just the stresses at a surface but in a volume to a depth of multiples of the precipitate dimension. One important point about Eqn. 5: the stresses in a minor phase can be very large and opposite in sign to a (small) stress in the major phase, and this can be quite important for example in crack initiation or stress corrosion.

Having defined the two kinds of stresses operationally, we turn now to the diffraction techniques to measure them. The basic idea is quite simple. The spacing of lattice planes acts as an internal elastic strain gauge; if the stress changes, the spacing changes, and a diffraction peak moves, as illustrated in Fig. 1. With x-rays, a few tens of microns can be probed, and in some cases, the stresses under a thick coat can be examined (4). By using glancing angle techniques, very thin layer of 30-100Å or so can be examined. As x-rays have an index of refraction slightly less than unity, total external reflection occurs at a few mrad; the refracted beam travels along the surface, acting as a source for diffraction from planes perpendicular to the surface to these small depths, Fig. 2. (The depth may be varied with this glancing angle.) For stresses in a surface these planes are more sensitive to the stress than planes parallel to the surface, which only "feel" the stresses through Poisson's effect. An example of such a study is shown in Fig. 3 for Al alloy film used as interconnect in solid state devices (5) For depths greater than a few tens of microns, glancing angles are not sufficient and layers must be removed.

With x-rays, portable field units are available and measurements can be done in seconds, if need be.

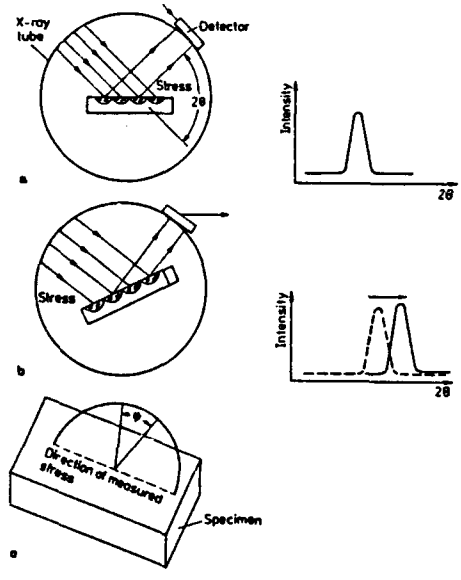


Figure 1. a) Schematic of diffractometer. The incident beam diffracts x-rays of wavelength $\lambda$ from planes that satisfy Bragg's law in crystals with these planes parallel to the sample's surface. If the surface is in compression, because of Poisson's ratio these planes are further apart than in the stress-free state. The d spacing is obtained from the peak in intensity versus scattering angle $2\theta$ and Bragg's law $\lambda = 2d\sin\theta$. b) After the specimen is tilted, diffraction occurs from other grains, but from the same planes, and these are more nearly perpendicular to the stress. These planes are less separated than in (a). The peak occurs at higher angles of $2\theta$. c) After the specimen is tilted, the stress is measured in a direction which is the intersection of the circle of tilt and the surface of the specimen.

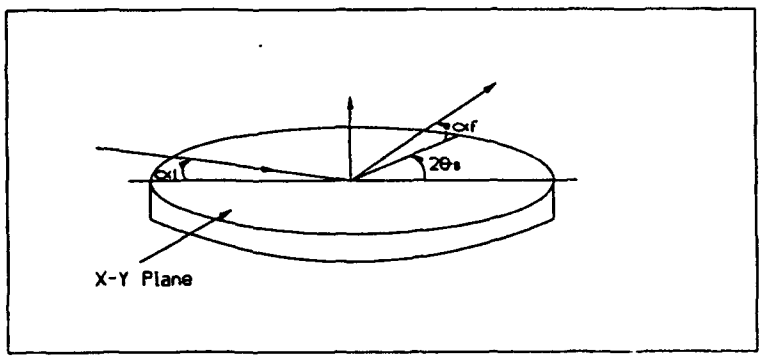


(a)

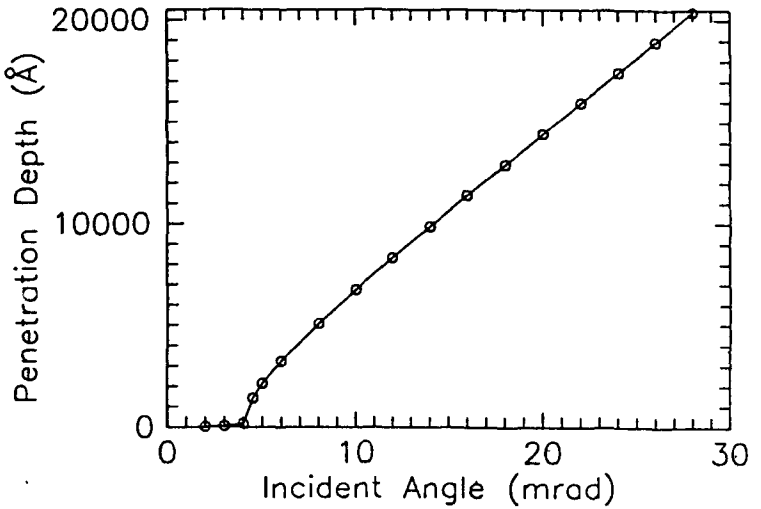


(b)

Figure 2: a) Geometry for glancing incidence diffraction. b) Penetration depth (1/e) vs. incidence angle. From Ref. 5.

The main advantage of using neutrons is the greater depth of penetration -- 10,000μm or so at least for most materials. Transmission techniques, are sometimes possible so that the planes most sensitive to the stress can be chosen. Because of such depths, the macrostresses usually average to zero, and only the microstresses are measured. However, if masks are employed, Fig. 4, the beam can be directed to sample only a small volume ( ~ 1 $mm^3$) and both kinds of stresses are measured. Smaller sampling regions are not possible, and even in this case, measurements take hours due to the weakness of neutron beams compared to x-rays -- and of course, access to a reactor is required. (Ref. 3 is an excellent book from a recent conference on the use of neutrons in stress determination.)

To properly sample a polycrystalline specimen, at least 2000 grains are required and even then the sample must be oscillated. For example, with x-rays, a 150μm beam can be employed if the grain size is 5μm. Smaller beam sizes require examination grain by grain.

Adequate sensitivity of ~10 MPa requires using reflections in the range of 150° 2θ, which precludes using electron diffraction.

Basic Theory

The sample is described in terms of co-ordinates $S_i$, as seen in Fig. 5. Measurements are made in the $L_i$ system, of the d spacing and hence the strain, ε, of planes perpendicular to $L_3$, at some sample tilt to the beam of $\phi,\psi$:

$$<\varepsilon^{\alpha}_{\phi\psi}> = \frac{<^{\alpha}_{\phi\psi}> - d^{\alpha}_{0}}{d^{\alpha}_{0}} = <\varepsilon^{\alpha}_{11}>\cos^2\phi\sin^2\psi + <\varepsilon^{\alpha}_{22}>\sin^2\phi\sin^2\psi$$
$$+ <\varepsilon^{\alpha}_{33}>\cos^2\psi + <\varepsilon^{\alpha}_{12}>\sin2\phi\sin^2\psi$$
$$+ <\varepsilon^{\alpha}_{13}>\cos\phi\sin2\psi + <\varepsilon^{\alpha}_{23}>\sin\phi\sin2\psi. \qquad (6a)$$

The trigonometric terms are simply those to rotate the rank two strain tensor in the $S_i$ system to the $L_i$ measuring system. Measurements are made over several ψ and φ and this equation is fit via least squares; the recommended values are $\phi = 0, 60, 120°$, and six ψ values to as high a value as possible (6). This maximizes the precision and minimizes any effects of steep gradients.

If the stresses are biaxial, $<\varepsilon^{\alpha}_{i3}> = 0$, and the "d" spacing is linear vs. $\sin^2\psi$. The value of $d_0$ is not needed in this case, as the stress value comes from the slopes vs. $\sin^2\psi$. If there are steep gradients, there is curvature in this plot, the same for ± ψ or $\phi = 0, 180, 340$, as well as 0, 60, 120°. If the $\sigma_{23}$, $\sigma_{13}$ terms are significant, these curves will differ. Finally, if the stresses vary greatly from point to point, due to elastic or plastic effects, there will be oscillations. If there is not much texture, the best line still gives the correct average value (7). If there is texture, the oscillations can be employed to give an indication of the range of strains (8).

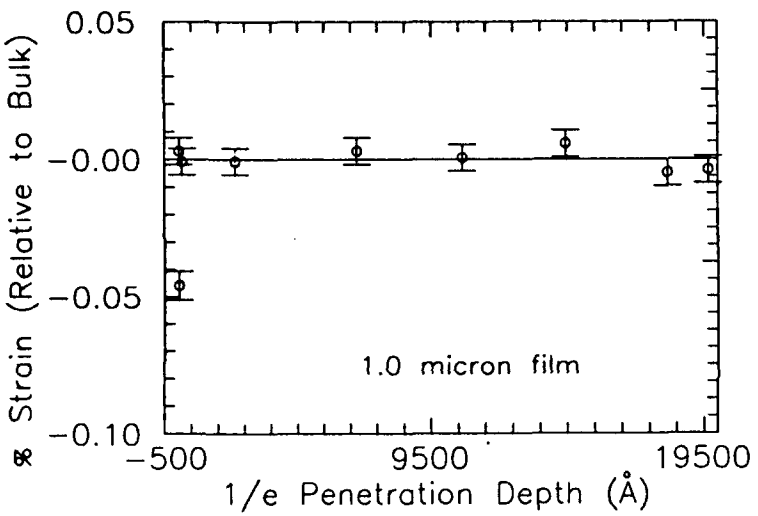


Figure 3. Relative percent strain (deviation from bulk) vs. penetration depth for Al-2%Cu, using glancing incidence x-ray diffraction, 1.0μm film on (001) Si wafer. From Ref. 5.

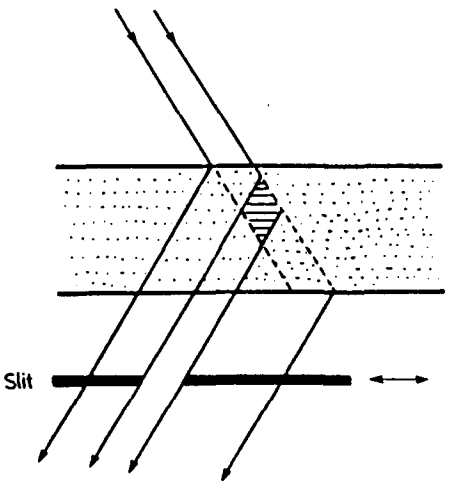


Figure 4. Neutron scattering. The beam penetrates the entire volume, but slits define a local volume. By moving the slits as shown, or the sample vertically, the stress in different volumes may be measured.

Therefore, it is clear that it is very important to measure d vs. $\sin^2\psi$. In the past, many people have assumed linearity and measured only two points. Obviously, with what we know now this is dangerous! Furthermore, it has been shown that several $\psi$ tilts can be examined in the same time as two tilts with the same or better precision (9).

From these strains the stresses may be calculated:

$$<^{I}\sigma_{ij}^{\alpha}>=\frac{1}{S_2/2}[<\varepsilon_{ij}^{\alpha}>-\delta_{ij}\frac{S_1}{S_2/2+3S_1}[<\varepsilon_{11}^{\alpha}>+<\varepsilon_{22}^{\alpha}>+<\varepsilon_{33}^{\alpha}>]] \quad (6b)$$

or combining 6a and 6b:

$$\begin{aligned}<\varepsilon_{\phi\psi}>= \; & \frac{S_2}{2}[<\sigma_{11}>\cos^2\phi+<\sigma_{12}>\sin 2\phi+<\sigma_{22}>\sin^2\phi]\sin^2\psi+ \\ & \frac{S_2}{2}<\sigma_{33}>\cos^2\psi+S_1[<\sigma_{11}>+<\sigma_{22}>+<\sigma_{33}>]+ \\ & \frac{S_2}{2}[<\sigma_{13}>\cos\phi+<\sigma_{23}>\sin\phi]\sin 2\psi. \end{aligned} \quad (7)$$

The x-ray elastic constants $S_1$ and $\frac{S_2}{2}$ can be calculated from the average of Voight and Reuss assumptions (10) or from Kröner's method (11) (an anisotropic grain in an isotropic matrix). Both give about the same result. If a sample is highly textured, it is best to measure these by applying known stresses in a jig on a diffractometer - in tension or bending (12).

Equations exist (9,12) for the errors in the resultant stresses and strains and it is important to use these. The error is not just that found from the best fit through the data, because each point has some statistical error and there are also errors in the elastic constants. In fact, based on these error equations, software has been developed for a PC (13) to determine stress (or elastic constants) to an operator-specified precision. It is difficult to be sure of the proper counting times without experience and such software minimizes wasted time. (Unfortunately, the available commercial software does not appear to properly take these errors into account!)

Determining a stress tensor in this way is sufficiently well established in a variety of materials that examples are not needed at this point. Nonetheless, some interesting possibilities exist when using diffraction to measure strains, that are particularly attractive, for thin films on brittle substrates, or for metal matrix composites. By following the "d" spacing while decreasing the temperature, it is possible to examine how tightly bound is the film or particle to its matrix, by making comparisons to known elastic solutions for this binding. If plastic yielding occurs, the d spacing will no longer change as only elastic strains are detected. An example is given in Fig. 6, where it is clear that the polycrystalline Al-Cu film on single crystal Si is fully bound, and the yield stress is

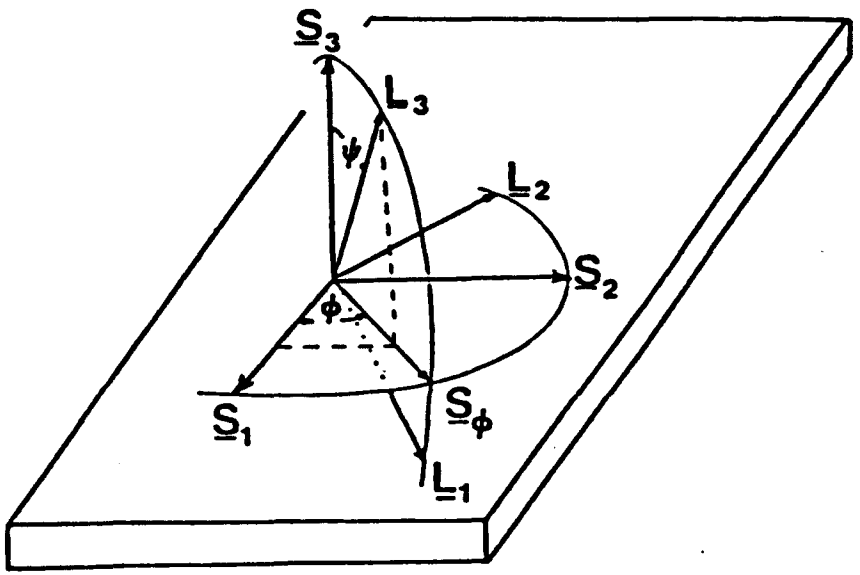


Figure 5. The coordinate system. The $S_i$ are the coordinates that describe the sample. The $L_i$ are the measuring coordinates. Diffraction from planes perpendicular to $L_3$ measures the change in spacing of these planes.

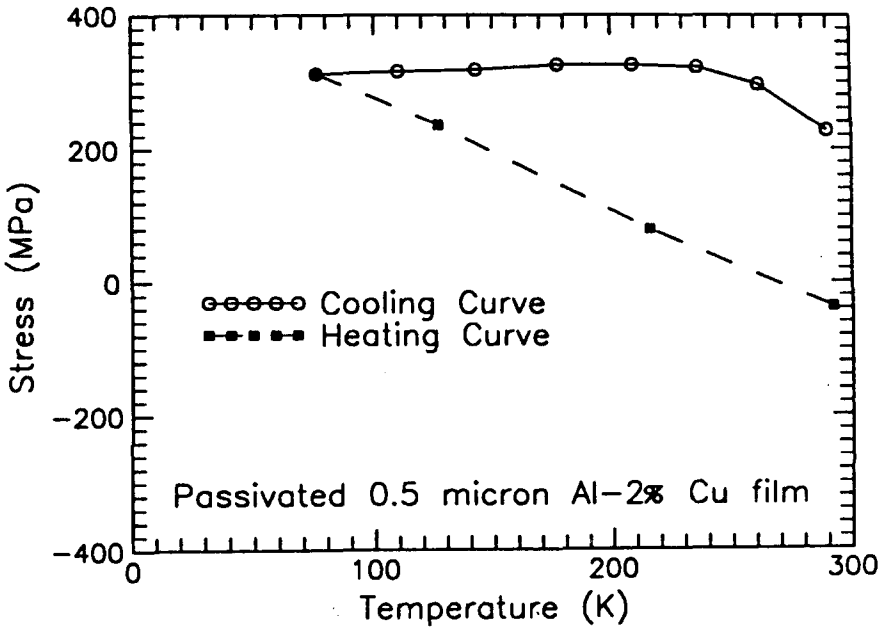


Figure 6. Cu film (001) Si wafer, from Ref. 14. The straight line portions are in agreement with complete bonding. The solid line turns horizontal at a stress of ≈300 MPa, the onset of plastic yielding.

clearly delineated (14). (The stresses arise in this case due to the different thermal contraction of the Si and alloy.)

The microstresses can also be examined by this cooling technique. A calculation can be made of the microstresses vs. temperature following Eshelby's equivalent inclusion procedure (15). The d spacing of a peak from either phase can then be followed as the temperature lowered. Two examples of this in ceramics composites are given in Fig. 7, by M. Oden, Linkoping University while visiting us. In SiC reinforced $Al_2O_3$ there are clearly microstresses, but in SiC-$TiB_2$ there are no stresses, probably because of local cracking. This was verified by actually measuring the stresses.

One word of caution on using this Eshelby calculation. Tsakalokos (16) has recently shown that if a particle is angular, the internal stresses are not constant, as is assumed in Eshelby's formulation. Such stresses due to differences in thermal contraction can also arise in composites and in a series of papers James, Marshall and co-workers have established this, making the particular point that measurements of the stresses are useful to validate modeling, because of the difficulty of including proper constitutive equations in such models and the many processes that can occur during the use of such materials. They have also found that:

a) In large-diameter fibers-reinforced metal matrix composites (large relative to beam penetration) the stress state at the surface is biaxial; there are significant gradients as the fiber interface is approached, and the stress state becomes triaxial (17,18).

b) There is a good comparison between stresses calculated from fiber-matrix interfacial sliding and from x-rays (19), which suggest that measured stresses may be useful in obtaining the interfacial (friction) shear stress.

c) Thermal or mechanical fatigue can lead to reductions in stress due to matrix deformation, or interfacial cracking. Stress measurements can be used to detect such effects (20). A similar effect was found by Hen and Predicki in $Al_2O_3$ fiber/glass composites (21). Furthermore, Ballard and Predecki (22) were able to measure the zero strain temperature in SiC reinforced $Al_2O_3$ (the temperature at which the thermal strains reverse on heating. If this is below the original processing temperature, some form of strain relief must have occurred.).

One vital note before proceeding: If the stress is truly hydrostatic, $\sigma_{11} = \sigma_{22} = \sigma_{33}$, there should be no $\phi$, or $\psi$ dependence of d. In this case, neutrons may be a better probe than x-rays. Due to the shallow x-ray penetration only the region of stress relaxation near the surface is seen (23). Triaxial analysis should be used if this is suspected, or neutrons.

Separating Micro and Macro Stresses

This is readily done for any number of phases. The stress tensor is measured in each phase and then Eq. 5 applied. In particular, for two-phases, $\alpha$ and $\beta$:

$$<{}^{I}\sigma_{ij}^{\alpha}> = {}^{M}\sigma_{ij} + <{}^{\mu}\sigma_{ij}^{\alpha}> \qquad (8a)$$

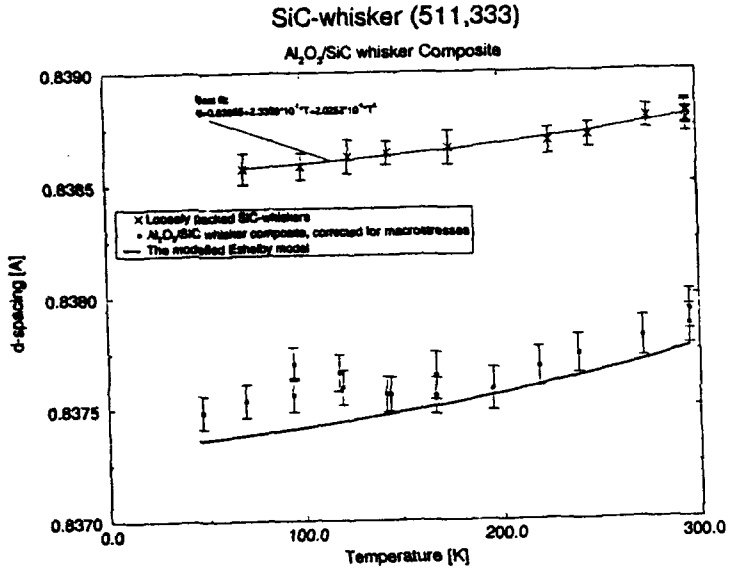


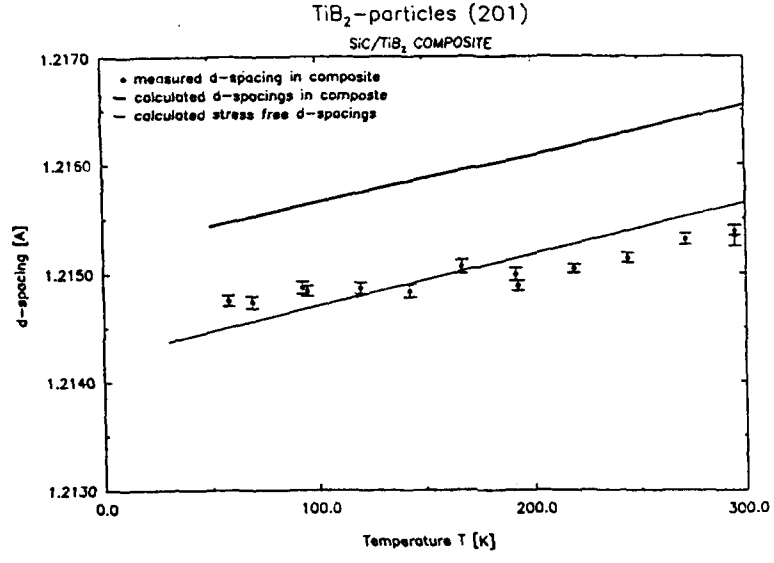


Figure 7(a) Cooling an $Al_2O_3$ /SiC carbide composite,(30 pct. vol SiC), compared to loose SiC powder. The data have been corrected for the measured macrostress tensor ~-85 MPa for $\sigma_{11}$ , $\sigma_{22}$. The dark solid line is from a calculation following Eshelby's method of equivalent inclusions.

(b). The same for SiC/$TiB_2$. composite. These measurements suggest that there is no stress and this was confirmed by measurement (± 13 MPa, close to the expected errors).
(M. Oden and J. B. Cohen, to be published.)

$$<{}^{t}\sigma_{ij}^{\beta}> = {}^{M}\sigma_{ij} + <{}^{\mu}\sigma_{ij}^{\beta}> \qquad (8b)$$

$$(1-f)<{}^{\mu}\sigma_{ij}^{\alpha}> + f<{}^{\mu}\sigma_{ij}^{\beta}> = 0. \qquad (8c)$$

The macrostress, ${}^{M}\sigma_{ij}$, is the same in all phases and therefore there are three unknowns in these three equations, permitting a solution for each component of the stress tensor, as first shown in Refs. 24,25. (See also Ref. 26). Alternatively, by using neutrons, and sampling the entire cross section, as mentioned above, only the microstresses are measured; then with a mask a smaller region can be sampled, involving both types of stress, and the macrostress determined by the difference of these two measurements (27).

This separation has been employed in a number of studies.

a) In a 60-40 brass, the matrix contained mostly macrostresses (25).

b) In 1080 steel, shot peening produces mainly macrostresses, whereas in simple extension mainly microstresses occur (28).

c) When a machined Sic-$TiB_2$ ceramic composite was bent (29), the microstresses generated by thermal mismatch during fabrication decayed, but not the macrostresses, signaling stress-induced microstress relief as the toughening mechanism. Thus, this local micro-cracking can be detected non destructively.

d) Carbon coatings on SiC fiber reinforcements in $Al_2O_3$ reduced the microstresses in the whiskers and the matrix (30,31).

Predicki, Abuhasan and Barrett (32) have shown that it is possible in some situations to obtain the microstresses in the fiber just from the stresses in the matrix. For example, ${}^{M}\sigma_{33} = 0$. Then the total $\sigma_{33}$ in the matrix is the microstress, ${}^{\mu}\sigma_{33}$. With Eqn. 5, the microstress in the fiber is obtained. This might prove particularly useful for non-crystalline fibers, or when there is severe fiber texture so that a useful fiber reflection is not available.

Eliminating The Need To Know The Unstressed Lattice Parameter

If the stress system is biaxial, this value isn't needed, but if it is triaxial, this is essential. In multiphase materials or composites, it is sometimes difficult to obtain this value; it is affected by fault density, composition; composition gradients, etc. and may be different in the bulk and in the composite, and great care is needed. However, a great deal of information can be obtained without this term, if we separate the stress components into deviatoric and hydrostatic terms. Following Winholtz (33) let:

$$\sigma_{ij} = \delta_{ij}\tau_H + \tau_{ij} \qquad (9)$$

The hydrostatic stress $\tau_H$ is given by:

$$\tau_H = (\sigma_{11} + \sigma_{22} + \sigma_{33})/3. \qquad (10)$$

The deviatoric stresses are given by:

$$\tau_{ij} = \sigma_{ij} : i \neq j$$
$$\tau_{ij} = \sigma_{ij} - \tau_H : i = j \qquad (11)$$

From equations 10 and 11 note that

$$\tau_{11} + \tau_{22} + \tau_{33} = 0 \qquad (12)$$

Substituting equations 6b, 9 and 12 into Eq. 7 and solving for $< d^{\alpha}_{\phi\psi} >$ gives:

$$\begin{aligned} <^{\alpha}_{\phi\psi}> = \quad & <^{t}\tau^{\alpha}_{H}> d^{\alpha}_{0}(S^{\alpha}_{2}/2 + 3S^{\alpha}_{1}) - (<^{t}\tau^{\alpha}_{11}> + <^{t}\tau^{\alpha}_{22}>) d^{\alpha}_{0} S^{\alpha}_{2}/2 + d^{\alpha}_{0} \\ & + <^{t}\tau^{\alpha}_{11}> d^{\alpha}_{0}(S^{\alpha}_{2}/2)(1 + \cos^2\phi)\sin^2\psi \\ & + <^{t}\tau^{\alpha}_{22}> d^{\alpha}_{0}(S^{\alpha}_{2}/2)(1 + \sin^2\phi)\sin^2\psi \\ & + <^{t}\tau^{\alpha}_{12}> d^{\alpha}_{0}(S^{\alpha}_{2}/2)\sin 2\phi \sin^2\psi \\ & + <^{t}\tau^{\alpha}_{13}> d^{\alpha}_{0}(S^{\alpha}_{2}/2)\cos\phi \sin 2\psi \\ & + <^{t}\tau^{\alpha}_{13}> d^{\alpha}_{0}(S^{\alpha}_{2}/2)\sin\phi \sin 2\psi. \end{aligned} \qquad (13)$$

Here we have $< d^{\alpha}_{\phi\psi} >$ (the parameter actually measured) in terms of the stresses in the sample and the unstressed lattice parameter for that phase. The term $<^{t}\tau^{\alpha}_{33}>$ has been eliminated using equation 12. As the deviatoric stresses vary with $\phi$ and $\psi$ while the hydrostatic stress does not, the deviatoric stress tensor can be determined by using the different angular dependencies using least squares techniques. Equation 12 is then used to get $<^{t}\tau^{\alpha}_{33}>$. Since it is simply a multiplier, errors in $d^{\alpha}_{0}$ will introduce only small errors in determining the deviatoric stresses. The hydrostatic stress, however, is contained in one of three terms that do not vary with $\phi$ and $\psi$. Only the sum of these three terms can be determined from the variation of $< d^{\alpha}_{\phi\psi} >$ with $\phi$ and $\psi$. In the first term, the hydrostatic stress is multiplied by elastic constants. Consequently, this term will be small in relation to $d^{\alpha}_{0}$ which is one of the other terms which does not vary with $\phi$ and $\psi$. Thus, the unstressed lattice spacing must be known very accurately in order to determine the hydrostatic component of the stress tensor while the deviatoric components of the stress tensor are relatively insensitive to it.

Equation 8 is also valid separately for separating the hydrostatic and deviatoric stress tensors into micro and macro components.

While it is desirable to know the entire stress tensor, the deviatoric stress tensor may be sufficient for many purposes, especially if the unstressed lattice parameters cannot be measured. If comparison measurements are to be made, for instance before and after a treatment, the difference in stress $\Delta\sigma$ will not contain any error due to errors in $d_0$. Also, if measurements are to be compared to a model calculation the deviatoric stresses may be sufficient to justify the model.

It is also worth noting that the deviatoric terms require only $\frac{S_2}{2}$ not $S_1$. Furthermore, the hydrostatic macrostress may be determined because ${}^{M}\sigma_{33} = 0$. Thus:

$$ {}^{M}\tau_{H} = -{}^{M}\tau_{33} \qquad (14) $$

In sum, all of the macro and micro deviatoric stress and the hydrostatic macrostress can be determined without knowledge of $d_0$, the unstressed lattice parameter.

This approach has been used to examine the load sharing in 1080 steel in low cycle fatigue (34). The development of stresses in a composite in a uniaxial test is illustrated in Fig. 8. Note that after unloading, the microstresses are different in different phases. After the fatigue hysterisis loop stabilized, the test was stopped at different points along the loop, the stresses measured and separated. The deviatoric microstresses were added to the applied stress tensor to give the stresses in each phase during fatigue, giving the result, for example, for the pearlitic condition, in Fig. 9.

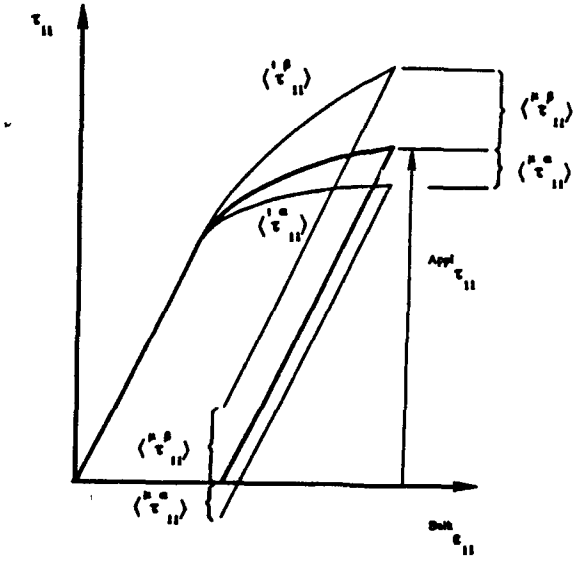

Figure 8. Mechanical behavior of a two phase material in a tensile test, assuming the same Young's modulus for both phases. The origin of the microstresses, in each phase on unloading is shown. From Ref. 34.

The pearlitic condition, spheroidite and tempered martensite were examined in this way and the authors used an Eshelby model to attempt to simulate the measurements. This model (which assumes non deforming inclusions) gave good results for the spherioditic condition, but the values were too high for pearlite, probably because the cementite deforms in this case. However, the model did predict that higher stresses and strain hardening would occur in the pearlite than in the spheroidite. For the martensite phase, the theory was in good agreement with results for the first cycle, but did not represent the increase in macrostresses on subsequent cycling.

Smith et al (35) have also looked at the residual microstresses for various morphologies in as produced SiC reinforced Al and found differences. Allen et al (36) examined the microstresses in this type of composite in tension and tested an Eshelby model against the results, again finding qualitative but not quantitative agreement -- in this case due to stress relaxation via plastic flow.

Stress Gradients

Throughout this text, brackets around stress components have often been employed to signal averaging over the depth of penetration. In effect

$$<\sigma_{ij}(P)>=\int_0^D \sigma_{ij}(t)\exp-(z/p)dz \Big/ \int_0^D \exp(-z/p)dz \qquad (15)$$

Here "P" represents the 1/e penetration depth, which for sample tilt $\psi$ around the omega axis is, for a mass absorption coefficient, $\mu$:

$$P = (\sin\alpha + \sin\beta)/\mu \sin\alpha \sin\beta) \qquad (16)$$

where $\alpha$ and $\beta$ are the incident and scattered angles. Predecki (37) has recently pointed out that for D larger than P (say 10P) the denominator is just P. Furthermore, if data is obtained vs. P (by grazing incidence for example, or the "d" spacing vs. $\sin^2\psi$), the strain or stress gradient might be obtained directly, because the numerator in Eq. 16 is a LePlace transform, and the inverse yields $\sigma_{ij}(t)$. It is only necessary to assume some reasonable mathematical form for $<\sigma_{ij}(P)>$. An actual example from this study is given in Fig. 10. This could prove to be an exciting development.

## Summary

Diffraction remains the premier tool for examining residual stresses non destructively, especially in composites. The entire stress tensor can be obtained, as well as the separate micro and macro stresses. The deviatoric macro and microstresses and hydrostatic macrostress can be sampled without knowledge of the unstressed lattice parameters of the phases, and by cooling the presence of microstreses can be determined, the strength of interface bonding and the yield stress of any phase. Via grazing incidence, gradients can be examined and there are new developments on this topic as well. The technique has more than kept pace with the needs of the research community as indicated by many papers in this conference.

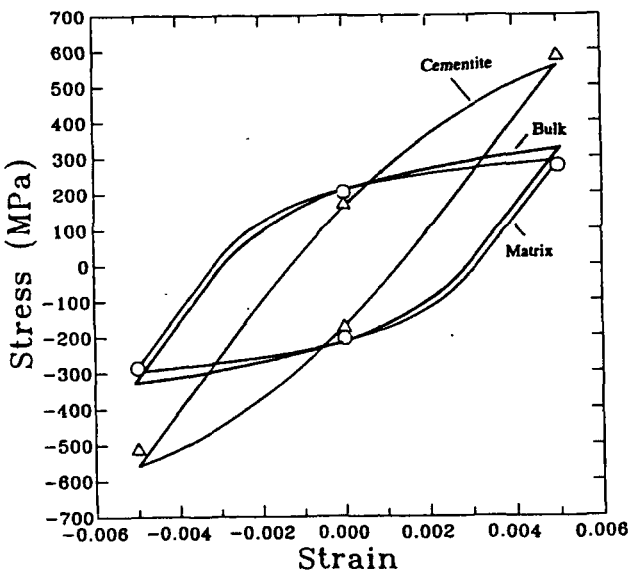


Figure 9. Hystersis loop for pearlitic 1080 steel, showing the sum of applied and microstreses in each phase. From Ref. 34.

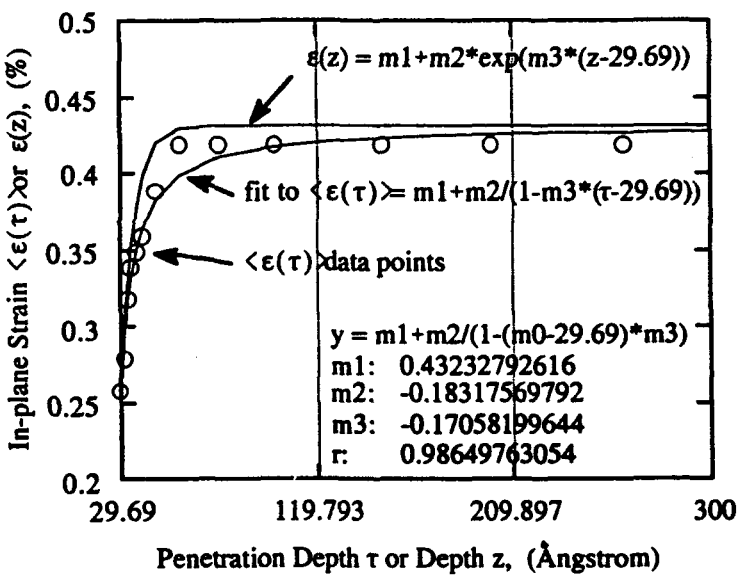


Figure 10. Circles are measurements of <ε(P)> = <ε(τ)> and the ε(z) determined from them by a reverse LaPlace transform, from Ref. 37.

## Acknowledgments

Our research in this area has been supported for many years by ONR and the many thoughtful comments and suggestions of our grant monitors, Dr. Bruce MacDonald (now at NSF) and Dr. George Yoder, have been much appreciated. I appreciate Prof. Predecki permitting me to describe his new technique for sampling gradients while it is still being developed.

I especially want to thank my former students in this area for their continued dialogue and friendship. I have probably learned more from them than they did from me and I am proud that they have become leaders in various aspects of this subject -- Prof. A. Krawitz in applying neutron diffraction, Dr. M. James in his studies of fiber reinforcement, Dr. I. C. Noyan in examining the effects of texture and thin films.

## References

1. I. C. Noyan and J. B. Cohen, "Residual Stresses in Materials", American Scientist, 79 (1991), 142-153.

2. I. C. Noyan and J. B. Cohen, Residual Stress Measurement by Diffraction and Interpretation, (New York: Springer-Verlag New York, Inc. 1987), 1-276.

3. M. T. Hutchings and A. D. Krawitz eds., Measurement of Residual and Applied Stress Using Neutron Diffraction, NATO ASI Series E: Applied Science, vol. 216 (Klurer Academic Publishers, Dondrecht, The Netherlands 1992) 1-588.

4. P. Georgopoulos, J. B. Cohen and H. Herman, "Residual Stress Measurements of a Plasma-Sprayed Coating System Using Synchrotron X-ray Radiation", Mat. Sci. & Engr., 86 (1986), L41-43.

5. C. J. Shute and J. B. Cohen, "Strain Gradients in Al-2%Cu Thin Films", J. Appl. Phys., 70 (1991), 2104-2110.

6. R. A. Winholtz and J. B. Cohen, "Generalized Least-Squares Determination of Triaxial Stress States by X-ray Diffraction and the Associated Errors", Aust. J. Phys., 41, (1988), 189-199.

7. I. C. Noyan, "The Theory of Stress/Strain Analysis", in Mat. Sci. & Engr., 86 (1986), 51-66.

8. R. H. Marion and J. B. Cohen, "Anomalies in Measurement of Residual Stress by Diffraction", Adv. in X-ray Anal., 18 (1975), 466-501.

9. M. R. James and J. B. Cohen, "Study of the Precision of X-ray Stress Analysis", Adv. in X-ray Anal., 20 (1977), 291-308.

10. H. Neerfeld, "The Calculation of Stress from X-ray Elongation Measurements", Mitt. KWI Eisentorsch., 24 (1942), 61.

11. E. Kröner, "Beerechinung der Elastischen Konstanten des Vielkristalls aus den Konstauten des Einkristalls", Z. Phys., 151 (1958), 504-508.

12. P. Rudnik and J. B. Cohen, "A Comparison of Diffraction Elastic Constants of Steel Measured with X-rays and Neutrons", Adv. in X-ray Anal., 31 (1988), 245-253.

13. A. Winholtz, "Microstresses and Macrostresses in the Fatigue of Steel", Ph.D. thesis, Northwestern University (1991).

14. C. J. Shute and J. B. Cohen, "Determination of Yielding and Debonding in Al-Cu Thin Films from Residual Stress Measurements via Diffraction", J. Mater. Res., 6 (1991), 950-956.

15. J. D. Eshelby, "The Determination of the Elastic Field of an Ellipsoidal Inclusion, and Related Problems", Proc. Roy. Soc., A241 (1957), 376-396.

16. S. S. Rao, T. Tsakalakos and W. R. Cannon, "Stress Distributions in Ceramic Composites Containing Faceted Inclusions", J. Amer. Cer. Soc., 75 (1992), 1807-1818.

17. M. R. James, "Residual Stresses in Metal Matrix Composites", in ICRS 2 (Elsevier Science Publishers LTD., Essex, England 1989), 429-435.

18. B. N. Cox, M. R. James, D. B. Marshall and R. C. Addison, Jr., "Determination of Residual Stresses in Thin Sheet Aluminum Composites", Met. Trans., 21A (1990), 2701-2707.

19. B. B. Cox, M. S. Dadkhah, M. R. James, D. B. Marshall, W. L. Morris and M. Shaw, "On Determining Temperature Dependent Interfacial Shear Properties and Bulk Residual Stresses in Fibrous Composites", Acta Metall. Mater., 38 (1990), 2425-2433.

20. M. R. James, "Behavior of Residual Stresses During Fatigue of Metal Matrix Composites", ICRS 3 (Elsevier Science Publishers, LTD, Essex, England, 1992), 555-560.

21. L. Hehn and P. Predecki, "Residual Stresses in Unidirectional $Al_2O_3$ Fiber Silicate Glass Composites by X-ray Diffraction", Adv. in X-ray Anal., 34 (1991), 669-677.

22. B. Ballard, P. Predecki and C. Hubbard, "Residual Strains in $Al_2O_3$ /SiC (Whisker) Composite From 25-1000°C", Adv. in X-ray Anal., 34 (1991), 465-471.

23. A. D. Krawitz, "The Use of X-ray Stress Analysis for WC-base Ceramics", Mat. Sci. & Engr., 75 (1985), 29-36.

24. I. C. Noyan, "Equilibrium Conditions for the Average Stress Measured by X-rays", Met. Trans., 14A (1983), 1907-1914.

25. I. C. Noyan and J. B. Cohen, "An X-ray Diffraction Study of the Residual Stress-Strain Distributions in Shot-Peened Two-Phase Brass", Mat. Sci. & Engr., 75 (1985), 179-193.

26. J. B. Cohen, "The Measurement of Stresses in Composites", Powder Diffraction, 1 (1986), 15-21.

27. L. Pintschovius, "Grain Interaction Stresses", in Measurement of Residual and Applied Stress Using Neutron Diffraction, NATO ASI Series E: Applied Science, vol. 216 (Klurer Academic Publishers, Dondrecht, The Netherlands (1992) 189-203.

28. R. A. Winholtz and J. B. Cohen, "Changes in the Macrostresses and Microstresses in Steel with Fatigue", Mat. Sci. & Engr., A154 (1992), 155-163.

29. D. J. Magley, R. A. Winholtz and K. T. Faber, "Residual Stresses in a Two-Phase Microcracking Ceramic", J. Amer. Ceram. Soc., 73 (1990), 1641-1644.

30. A. Abuhasan and P. K. Predecki, "Residual Stresses in $Al_2O_3$/SiC (Whisker) Composites Containing Interfacial Carbon Films", Adv. in X-ray Anal., 32 (1989), 471-479.

31. A. Abuhasan, C. Balasingh and P. Predecki, "Residual Stresses in Aluminum/Silicon Carbide (Whisker) Composites by X-ray Diffraction", J. Amer. Cer. Soc., 73 (1990) 2474-2484.

32. P. Predecki, A. Abuhasan, and C. S. Barrett, "X-ray Elastic Constants for β-SiC and Residual Stress Anisotropy in a Hot-Pressed $Al_2O_3$/SiC (Whisker) Composite", Adv. in X-ray Anal., 34 (1991), 643-650.

33. R. A. Winholtz, "Separation of Microstresses and Macrostresses", Mat. Sci. & Engr., 86 (1986), 131-146.

34. R. A. Winholtz and J. B. Cohen, "Load Sharing of the Phases in 1080 Steel During Low-Cycle Fatigue", Met. Trans., 23A (1992), 341-354.

35. L. F. Smith, A. D. Krawitz, P. Clarke, S. Saimoto, N. Shi and R. J. Arsenault, "Residual Stresses in Discontinuous Metal-Matrix Composites", Mat. Sci. & Engr., in press.

36. A. J. Allen, M. A. Bourke, S. Daves, M. T. Hutchings and P. J. Withers, "The Analysis of Internal Strains Measured by Neutron Diffraction in Al/SiC Metal Matrix Composites", Acta. Metall. Mater., 46 (1992), 2361-2373.

37. P. Predecki, "Determination of Depth Profiles from X-ray Diffraction Data", in preparation.

Security Classification

## DOCUMENT CONTROL DATA - R & D

*(Security classification of title, body of abstract and indexing annotation must be entered when the overall report is classified)*

| 1. ORIGINATING ACTIVITY (Corporate author) | 2a. REPORT SECURITY CLASSIFICATION |
|---|---|
| J. B. Cohen<br>McCormick School of Engineering<br>Northwestern University<br>Evanston, IL 60208 | 2b. GROUP |

3. REPORT TITLE

SOME RECENT RESULTS ON STRESSES IN THIN FILMS AND PRECIPITATES

4. DESCRIPTIVE NOTES (Type of report and inclusive dates)

TECHNICAL REPORT 33

5. AUTHOR(S) (First name, middle initial, last name)

J. B. Cohen

| 6. REPORT DATE | 7a. TOTAL NO. OF PAGES | 7b. NO. OF REFS |
|---|---|---|
| | 18 | |

| 8a. CONTRACT OR GRANT NO. | 9a. ORIGINATOR'S REPORT NUMBER(S) |
|---|---|
| b. PROJECT NO. | 33 |
| c. | 9b. OTHER REPORT NO(S) (Any other numbers that may be assigned this report) |
| d. | |

10. DISTRIBUTION STATEMENT

Distribution of document is unlimited

| 11. SUPPLEMENTARY NOTES | 12. SPONSORING MILITARY ACTIVITY |
|---|---|
| | Metallurgy Branch<br>Office of Naval Research |

13. ABSTRACT

Diffraction remains the premier tool for sampling the residual stresses in materials non destructively, the only one capable of determining the entire stress tensor, and with few assumptions. The technique has kept pace with the needs of researchers in the area of multiphase materials; now, the stresses can be separated into macro and micro components. The deviatoric macro and micro stress components and hydrostatic macrostress can be measured without knowledge of the unstressed lattice parameter. Bond strength of film and fiber and the yield stress can be examined by cooling samples, and there are new developments that enable gradients to be determiend.